IVS Memorandum 2007-002v01

9 April 2007

"CONT05 B"

Alessandra Bertarini, Brian Corey,
Kerry Kingham, Alan Roy

CONT05 B

A. Bertarini, B. Corey, K. Kingham, A. L. Roy

April 2007

1 Introduction

To ease the comparison between the CONT05 data and those from other non-VLBI techniques it was decided to re-fringe fit the whole campaign to shift the boundaries between the sessions from 17 UT to 0 UT. That implied concatenating contiguous experiments by changing the *fourfit* control files and adapting them to suit each pair of newly joined sessions. The idea developed further, that since re-fringe fitting was needed, then it might be possible to measure the earth orientation paramenters (EOP) variabilities on the time-scales between hours to 15 days if one global *fourfit* control file was used. The aim of this memo is to describe the steps taken during the re-fringe fitting and the difficulties encountered in the process. The re-fringe fitting took place at the Bonn correlator with the support of the Haystack and Washington correlators.

2 Verification Steps

To demonstrate that it might be possible to fringe fit the whole 15-day-long CONT05 campaign with one control file, we took CONT0501, the first of the series and CONT0515, the last of the series and performed a trial fringe fitting using the CONT0508 *fourfit* control file. A control file specifies the parameters used by the program *fourfit* to control the fringe fitting process. The parameters that can influence the geodetic observable are listed below:

- Start and stop time: scan start and stop time offset for the data to be considered valid and so included.
  This parameter can influence the geodetic observables if some bad data are allowed to pass. In the CONT05, there were very strong spurious fringes in the first AP almost dominating the fringes from the radio source in some low-fringe-rate scans. These spurious signals were a known artifact created by the station units if the scan start time is equal to the recording start time as was the case for CONT05 and needed to be removed from the analysis.

- *dr_win*: delay-rate search window bounds, in μs.
  The choice of this parameter can affect which peak is selected.

- *lsb_offset*: additive phase in degree for the lower sideband (LSB) relative to the upper sideband (USB).
  It is often necessary when correlating VLBA data against Mark 4 data to correct a constant offset.

- *pc_freqs*: specify which of the phase cal tones that were extracted by the correlator should be used for the analysis.
  These parameters were set to have the same values for the different stations. This parameter is needed to calibrate the visibility phases across the frequency channels.

- *pc_mode*: specify whether the phase_cal mode is normal (the phase cal phases are added to the visibility phases) or manual (the phase cal phases are not added to the visibility phases).

- *pc_phases*: specify a list of phases to be added to the fringe visibilities in each frequency channel if pc_mode is normal.

In the original fringe-fitting, different values of all these parameters, except for lsb_offset, pc_freq and pc_mode were used in the control files for the different sessions. In the global control file all these parameters were set to fixed values throughout all the sessions.

The validation tests consisted of comparing the SNR and the spectral coherence (rms of the phases across the spanned RF bandwidth) of the highest SNR scans on each baselines from the original fringe fit and from the re-fringe fit. Figures 1 and 2 show the results of the validation tests, which were positive. The top plot in Fig. 1 shows the X-band SNR of some scans of CONT0501 as fringe-fitted with its *fourfit* control file (labelled in the figure as c0501) and with the CONT0508 *fourfit* control file shifted up by 300 units for clarity (labelled as c0508 + 300). The two curves are almost identical. The difference is shown in the lower plot in Fig. 1 on an expanded vertical scale. Fig. 2 shows the X-band spectral coherence of some scans of CONT0515 as fringe-fitted with its *fourfit* control file (labelled in the fig as c0515) and with the CONT0508 *fourfit* control file shifted up by 10 units for clarity (labelled as c0508 + 10). As for the SNR comparison, the two curves are almost identical and the difference is shown in the lower plot on an expanded vertical scale. The change in additive phases between the single control files and the global was at most of 3° within one frequency channel.

3 Analysis

After we demonstrated that it was likely we could re-fringe fit the whole session with one control file all the correlated data from CONT05 sessions were transferred via FTP to Bonn for the analysis. It quickly became apparent that there were many residual MBD jumps and the first issue became to have the fewest clock jumps as possible. Clock jumps seen in the residual MBD originated

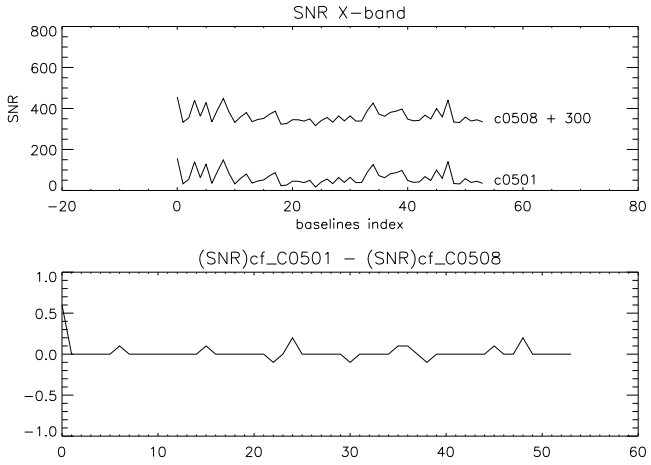

Figure 1: Above: SNR for the highest SNR scans of CONT0501 extracted from the files fringe-fitted with C0501 (c0501) *fourfit* control file and C0508 (c0508 + 300) *fourfit* control file shifted of 300 units. Below: difference of the SNRs between the CONT0501 data fringe fitted with C0501 *fourfit* control file and C0508 *fourfit* control file.

mostly from the different clock models used at the correlators for each session and from the resetting of the phase cal (pcal) generator. Both kinds of jump happened almost always simultaneously at session boundaries. The boundaries jumps due to clock models represent no problem since for every jump seen in the residual MBD there will be a corresponding jump of the opposite sign in the clock model, and the total delay (residual plus model) will show no jump. The jumps generated by the pcal generator (from now on, pcal jumps) were not accounted for in the model and so affected the total delay and therefore needed to be carefully located and removed. The pcal jumps were a concern in the S-band because the spacings between the channels were not integer multiples of 5 MHz. The pcal jumps were not a concern in X-band because the spacings among channels were integer multiple of 5 MHz.
The pcal generator takes the 5 MHz sinusoidal signal from the maser and generates a train of sharp pulses with a spacing of 0.2 μs. In the frequency domain, the output is a comb with spacing of 5 MHz extending to very high frequency. For geodetic VLBI we use a comb spacing of 1 MHz. To produce this narrower comb spacing, the pcal generator contains a gate that passes one in five of the pulses, thus outputting a pulse each 1 μs. To implement this mode, the pcal generator contains a counter which counts up to five, opens the gate to allow through a pulse, and resets the counter. If the pcal generator is reset or a power failure happens, then the counter loses track of the count and starts again from zero. This causes delay jumps of 0.2 μs, 0.4 μs, 0.6 μs, or 0.8 μs. Once the

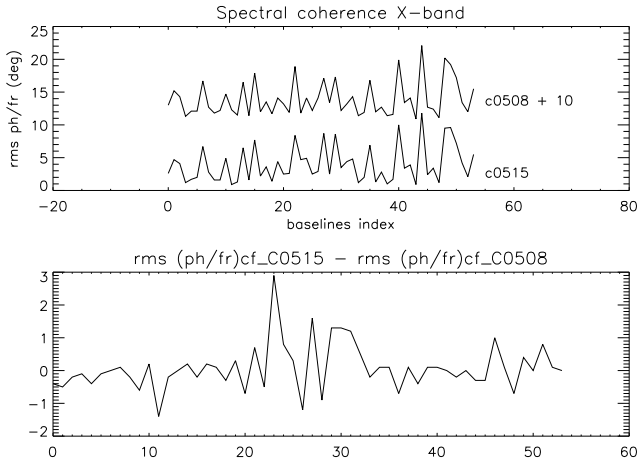

Figure 2: Above: Spectral coherence for the highest SNR scans of CONT0515 extracted from the files fringe-fitted with C0515 (c0515) *fourfit* control file and C0508 (c0508 + 10) *fourfit* control file shifted of 10 units. Below: difference of the spectral coherence between the CONT0515 data fringe fitted with C0515 *fourfit* control file and C0508 *fourfit* control file.

pcal are applied to the data (this is done in the fringe fitting stage by *fourfit*), the delay jumps introduce jumps in the MBD. Fortunately the pcal jumps leave a characteristic signature in the data: the phase cal difference relative to the first channel will jump by particular integer multiples of 72°. The jumps can be calculated starting from the formula

$$\tau = \frac{\Delta\phi}{\Delta\nu} \tag{1}$$

and are reported in Table 1.

For example, Fig. 3 shows the phase cal phase difference for all BBCs vs time for a station that interrupted the the power to the pcal generator periodically. The jumps are integer multiples of 72° and are different for each channel, following the pattern described in Table 1. Fig. 4 shows the same for a station that did not interrupt the power. The jumps in Fig. 4 are 360° wraps in the display and so do not represent a problem.

To double check that the pcal jumps do indeed affect the residual MBD as expected, we plotted the residual MBD vs time and saw numerous MBD jumps. Some of these jumps occurred at pcal jumps and others when the correlator clock model changed at sessions boundaries. To show the pcal jumps more clearly, we removed the jumps due to clock model breaks by adding back in the clock models taken from the ovex files. The result for a good station is shown in Fig. 5. The addition of the clock model produced a constant drift in the

Table 1: Phase jumps expected for given frequency differences between BBCs and given pcal delays jump sizes.

$\Delta\nu$	0 MHz	8 MHz	24 MHz	80 MHz	112 MHz	120 MHz	MBD jumps after wrapping at 0.125 μs
$\Delta\phi$ for MBD jumps of 0.2 μs	0°	216°	288°	0°	144°	0°	0.075 μs
$\Delta\phi$ for MBD jumps of 0.4 μs	0°	72°	216°	0°	288°	0°	0.025 μs
$\Delta\phi$ for MBD jumps of 0.6 μs	0°	288°	144°	0°	72°	0°	0.10 μs
$\Delta\phi$ for MBD jumps of 0.8 μs	0°	144°	72°	0°	216°	0°	0.05 μs

residual MBD plus clock due to the station clock rate. The results for a station with pcal jumps is shown in Fig. 6. In Fig. 6 it seems that the pcal jumps are always less than 0.2 μs; this is due to the modulo 0.125 μs ambiguities spacing of the S-band frequency sequence, which wrap the delays (and so the pcal jumps) into the range between $\pm$0.0625 μs (see Table 1 column 8).

After all the pcal jumps were recognized, we wrote a global *fourfit* control file with which to re-fringe fit the whole campaign. The additive phases for the global *fourfit* control file were constructed from those in the single-session *fourfit* control files in one of three ways, depending on whether the station was good, had pcal jumps, or required manual pcal. For good stations, we averaged the additive phases from the individual *fourfit* control files for the global *fourfit* control files. For stations with pcal jumps, we used the additive phases from the *fourfit* control file of the first session and at the time of each pcal jump we added to the additive phase the appropriate multiples of 72° from Table 1 required to remove the resulting delay jumps. For the one station requiring manual pcal (Kokee Park), we saw that the manual phases applied in the single sessions were very close to each other, so we took the CONT0506 values and applied them to the whole campaign. At the end of the fringe fitting, we performed the same verification checks as described in section 2. We took CONT0501, CONT0506 and CONT0513 and checked the SNR, spectral coherence and MBD. The results are shown in Figs. 7, 8 and 9 and gave us confidence that the process of fringe fitting all sessions with one global *fourfit* control file worked well. The effect on the MBD of fringe fitting with one global file cannot be easily determined for every single change separately because all the changes were applied in one run of fringe fit. In almost 17500 measurements in CONT0501, CONT0506 and CONT0513, the results of all the changes made a change in the MBD of less than 7.8 ps rms except for the six outliers, a change in spectral coherence of

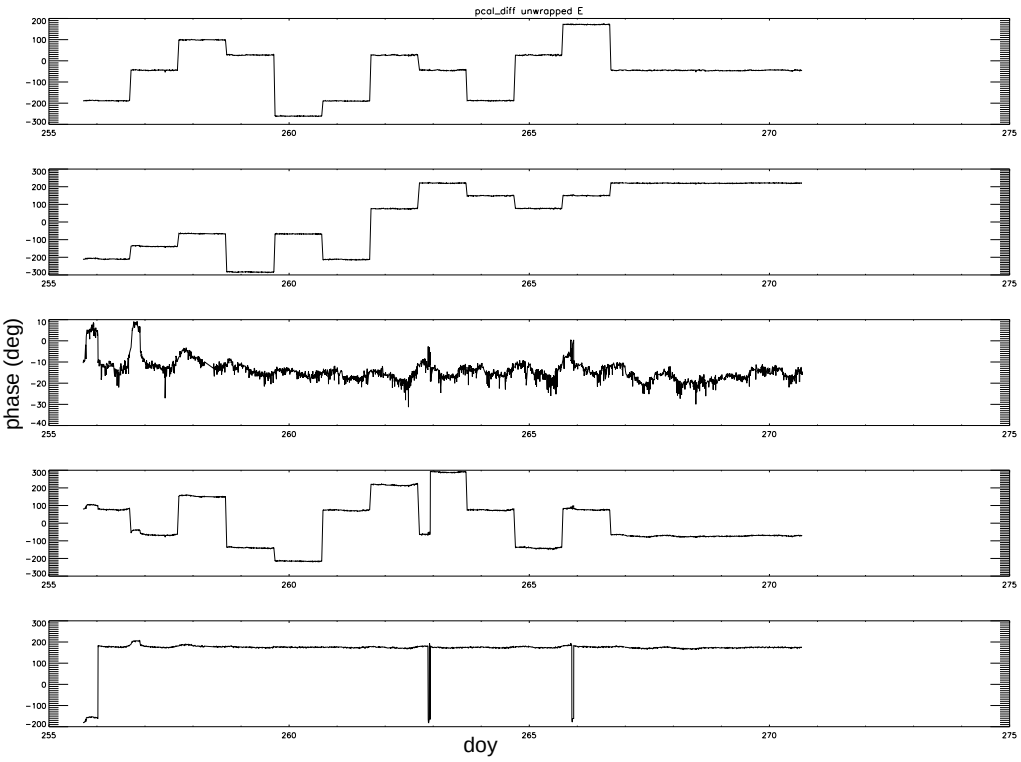

Figure 3: From top to bottom: phase cal difference between the first S-band channel and each of the other S-band channels vs time for a station that interrupted the pcal generator between each session up to doy 266. The abscissas are the doy and the ordinates are the phase cal phase difference in degree Note: the y axes are automatically rescaled. The reference BBC is at 2232 MHz and the $\Delta\nu$ displayed top to bottom are at 8 MHz, 24 MHz, 80 MHz, 112 MHz and 120 MHz.

1.03° rms (same six outliers) and a change in SNR of 2.8 rms (same six outliers).

4 Conclusion

It was found possible to use a global *fourfit* control file to fringe fit all the CONT05 sessions without noticeable loss of SNR or spectral coherence and without affecting the residual MBD significantly. Each pcal jump caused by cycling power to the pcal generator at some stations had to be recognized by hand and corrections calculated and introduced into the additive phase offsets. This was found to work well, though was time consuming. The system, choosing to observe at frequencies that are integer multiples of 5 MHz, is robust to pcal

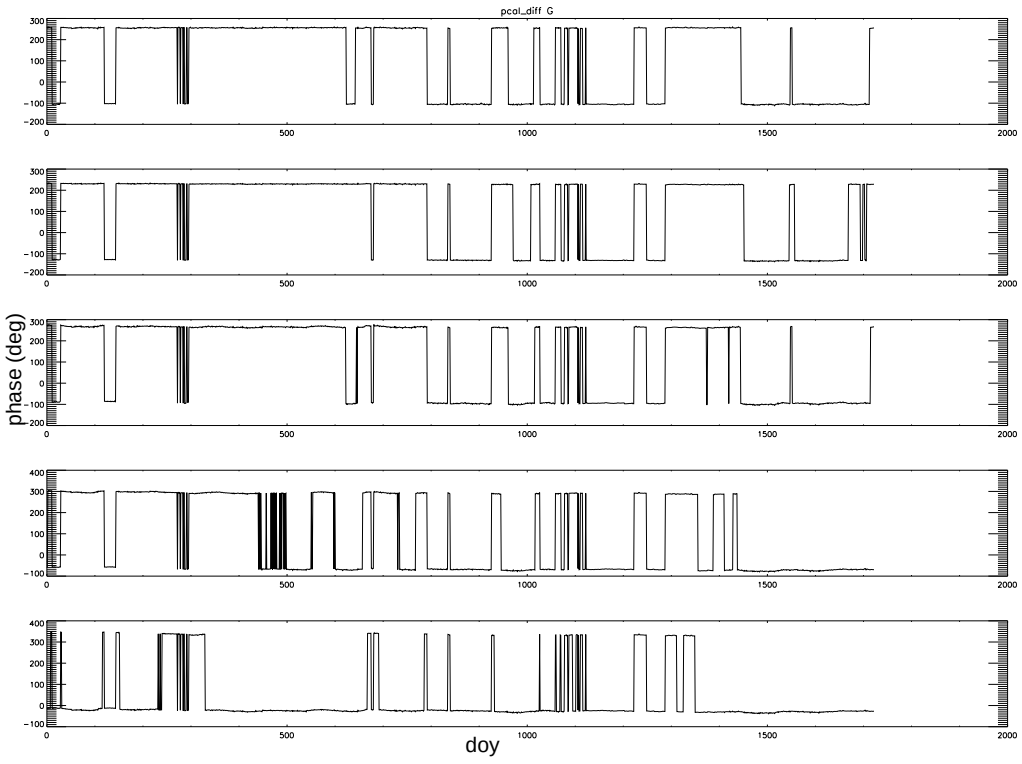

Figure 4: From top to bottom: phase cal difference between the first S-band channel and each of the other S-band channels vs time for a station that did not interrupt the pcal generator.The jumps are 360° phase wraps. The BBC frequencies are as for Fig. 3

jumps. All CONT05 sessions were re-fringe fitted with a global *fourfit* control file and the resulting database was submitted to the data centres for the analysis as CONT05 B. Using those data it should be possible to follow inter-session EOP variations without complications from changing *fourfit* control file parameters from session to sessions.

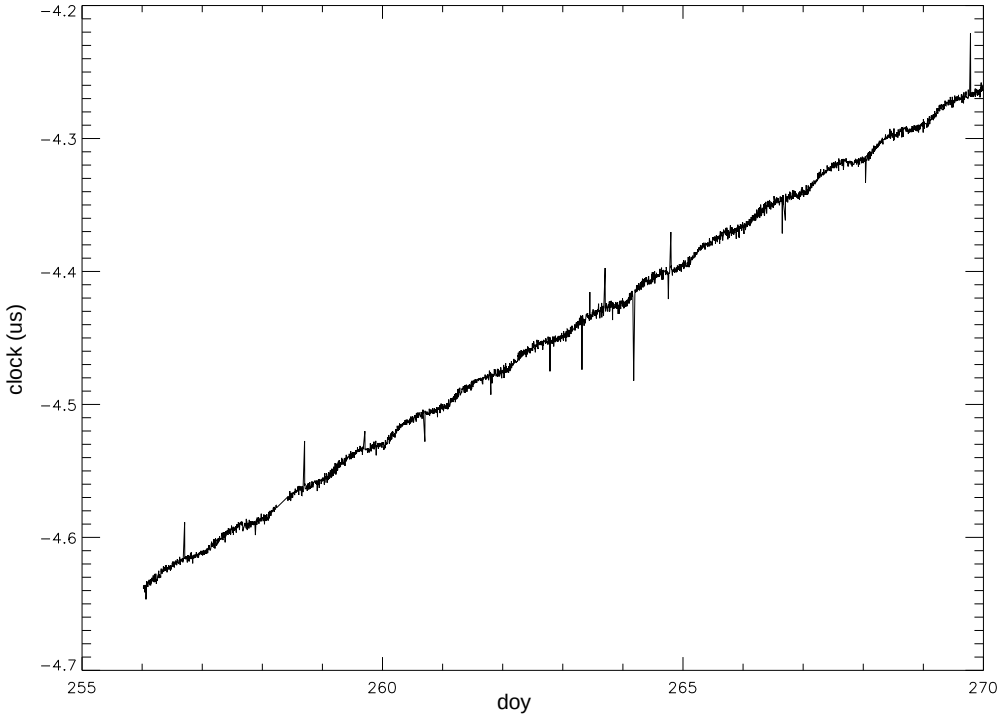

Figure 5: MBD vs time for a good station throughout the whole CONT05 after adding back the clock models that had been applied at the various correlators. The result is a uniform drift due to the station clock rate and shows no breaks.

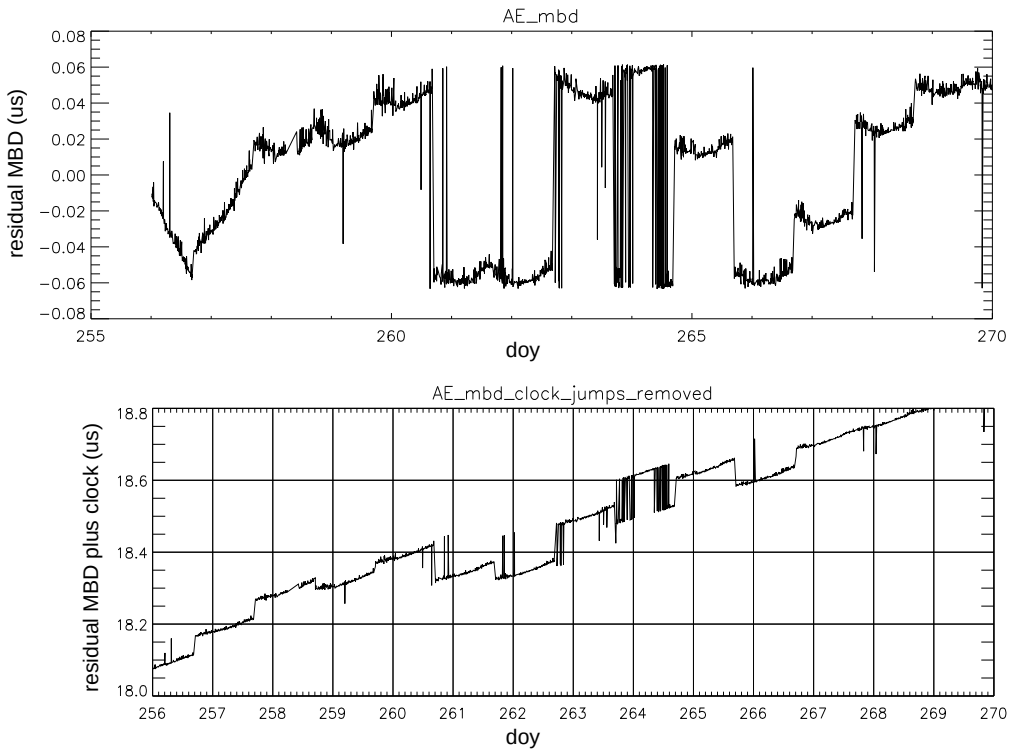

Figure 6: Top: residual MBD vs time through the whole CONT05 for a station that interrupted the pcal. Jumps in the residual MBD are caused by pcal interruptions and discontinuities at session boundaries due to different clock models used at different correlators. Bottom: same as the top plot, but after adding back in the clock models from the ovex files used at the different correlators. This removes the discontinuities at session boundaries due to different clock models, and leaves the station clock rate visible as an overall slope. The remaining step discontinuities are those due to interruption of the pcal.

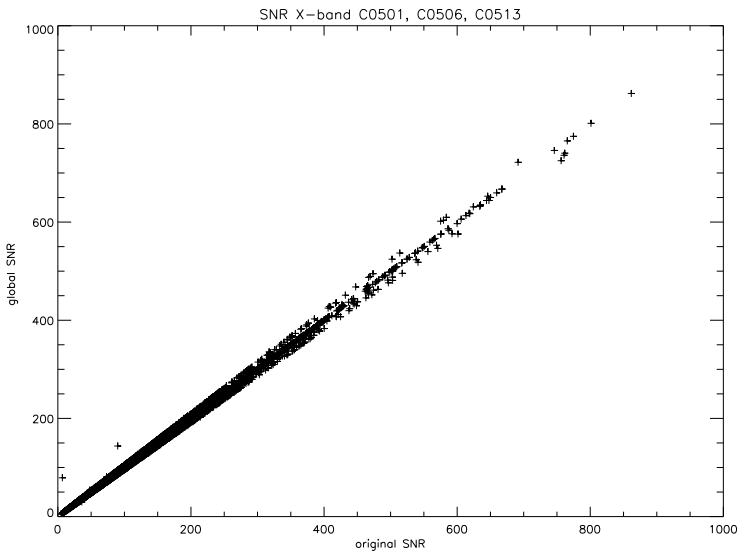

Figure 7: SNR comparison between the CONT0501, CONT0505 and CONT0513 fringe fitted with single *fourfit* control files (abscissa) and CONT0501, CONT0505 and CONT0513 fringe fitted with the global *fourfit* control file (ordinate). No significant change in SNR was caused by using the global *fourfit* control file. The rms change of SNR is 2.6.

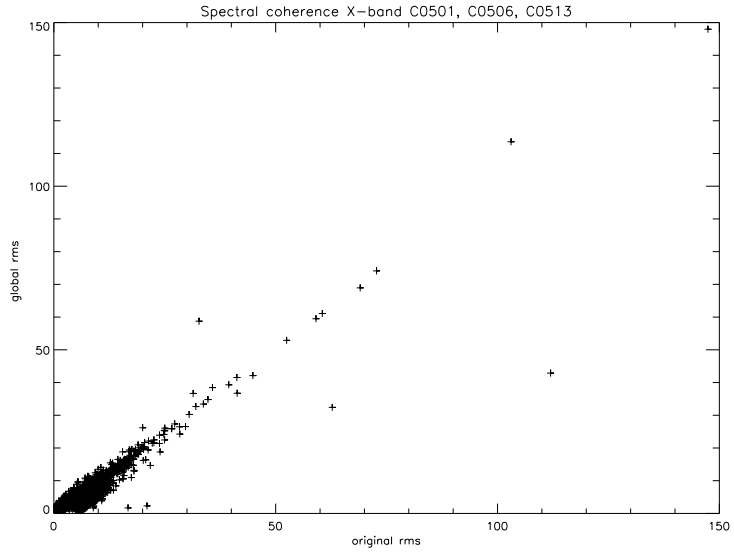

Figure 8: Spectral coherence comparison between the CONT0501, CONT0505 and CONT0513 fringe fitted with single *fourfit* control files (abscissa) and CONT0501, CONT0505 and CONT0513 fringe fitted with the global *fourfit* control file (ordinate). The majority of scans were not significantly affected by using the global *fourfit* control file. The scans lying below the 45° line showed improved spectral coherence from using the global *fourfit* control file due to errors that were detected in the individual *fourfit* control files and were corrected in the global *fourfit* control file. The scans lying above the 45° line showed degraded spectral coherence from using the global *fourfit* control file. Axis units are degrees. After the removal of the six outliers the rms change in spectral coherence is 1.03°.

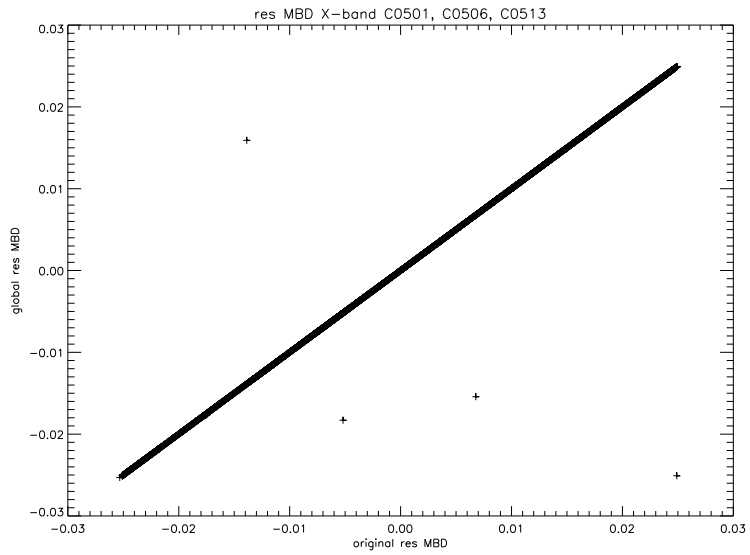

Figure 9: MBD comparison between the CONT0501, CONT0505 and CONT0513 fringe fitted with single *fourfit* control files (abscissa) and CONT0501, CONT0505 and CONT0513 fringe fitted with the global *fourfit* control file (ordinate). The majority of scans were not significantly affected (7.8 ps rms change in MBD). Axis units are μs.